ELSEVIER

Journal of Power Sources 114 (2003) 113–120

JOURNAL OF POWER SOURCES

www.elsevier.com/locate/jpowsour

Nanocrystalline tin oxides and nickel oxide film anodes for Li-ion batteries

Yan-Na Nuli, Sheng-Li Zhao, Qi-Zong Qin*

Department of Chemistry, Laser Chemistry Institute, Fudan University, Shanghai 200433, PR China

Received 22 March 2002; received in revised form 29 July 2002; accepted 26 September 2002

Abstract

Tin oxides and nickel oxide thin film anodes have been fabricated for the first time by vacuum thermal evaporation of metallic tin or nickel, and subsequent thermal oxidation in air or oxygen ambient. X-ray diffraction (XRD) and scanning electron microscopy (SEM) measurements showed that the prepared films are of nanocrystalline structure with the average particle size <100 nm. The electrochemical properties of these film electrodes were examined by galvanostatic cycling measurements and cyclic voltammetry. The composition and electrochemical properties of SnO_x ($1 < x < 2$) films strongly depend on the oxidation temperature. The reversible capacities of SnO and SnO_2 films electrodes reached 825 and 760 mAh g^{-1}, respectively, at the current density of 10 μA cm^{-2} between 0.10 and 1.30 V. The SnO_x film fabricated at an oxidation temperature of 600 °C exhibited better electrochemical performance than SnO or SnO_2 film electrode. Nanocrystalline NiO thin film prepared at a temperature of 600 °C can deliver a reversible capacity of 680 mAh g^{-1} at 10 μA cm^{-2} in the voltage range 0.01–3.0 V and good cyclability up to 100 cycles.

Keywords: Li-ion batteries; Thin films; Tin oxide; Nickel oxide; Vacuum thermal evaporation

1. Introduction

Nano-sized metal oxides as anode materials for lithium-ion batteries have been intensively investigated recently. Among them, tin oxides such as SnO, SnO_x ($1 < x < 2$) and SnO_2 have been proven to be promising anodes since the compounds containing Li-alloying metals can deliver much higher reversible capacities than graphite and generally have better cycle stability than the respective metal hosts [1]. In addition, tin oxides are stable in air and non-aqueous electrolytes. However, the reduction of the SnO with Li to metallic Sn and Li_2O during the first cycle and the very large change in volume during charge and discharge cause the internal damage to the electrode and an irreversible conversion reaction resulting in a significant loss of capacity [2]. Recently, it has been pointed out that electrodes composed of nanocrystalline particles exhibit high capacity and better cyclability [3,4]. For instance, a nano-structured SnO_2-based electrode can deliver very high capacity (~700 mAh g^{-1} at a rate of 8C) and still retain the ability to be discharged and recharged for 800 cycles [5]. Besides tin oxides, anode electrodes made of nano-sized transition-metal oxides (MO, where M is Co, Ni, Fe or Cu) have been reported by Tarascon and co-workers [6]. These electrodes exhibited electrochemical capacities as high as 700 mAh g^{-1} with a 100% capacity retention up to 100 cycles. They proposed a new mechanism, which is different from the Li-alloying processes for the tin oxide based anodes, involves the reversible formation and decomposition of Li_2O, accompanying the reduction and oxidation of metal nanoparticles of 1–5 nm. These investigations have led to a renewed interest in using nano-sized metal oxides as promising anode materials for rechargeable Li-ion batteries.

Rechargeable thin film batteries have been considered a promising power source for many applications, such as smart cards, micro-devices and portable electronics. Until now Li-metal film has usually been used as an anode material, but it is very unstable due to its high reactivity and low melting point. The use of tin oxide films as alternative anode materials may overcome these disadvantages. Tin oxide films have been prepared by various methods such as sputtering [7], spray method [8], chemical vapor deposition (CVD) [9], e-beam evaporation [10,11] and sol–gel technique [12]. We have reported the fabrication of the thin

* Corresponding author. Tel.: +86-21-6510-2777; fax: +86-21-6510-1515.
E-mail address: qzqin@fudan.ac.cn (Q.-Z. Qin).

0378-7753/02/$ – see front matter
PII: S0378-7753(02)00531-1

films of tin composite oxide (TCO) and NiO as anode materials with excellent electrochemical properties by reactive pulsed laser deposition (PLD) [13,14]. However, the lack of uniformity of the deposited film over a large area is one of the major drawbacks of PLD technique.

It is well known that vacuum thermal evaporation and subsequent thermal oxidation has proven to be a simple and efficient method to fabricate smooth and dense thin films over a large area. In this work, we used this method to fabricate thin films of nanocrystalline tin oxides and nickel oxide. The influence of thermal oxidation temperature on the composition and electrochemical properties of thin film electrodes was examined. We hope to provide an alternative method in fabricating anode film electrodes with high capacity and good cycling performance for all-solid-state thin film Li-ion batteries.

2. Experimental

Sn and Ni thin films were firstly prepared by thermal evaporation onto stainless-steel substrates or Si substrates in a deposition chamber evacuated to 10^{-6} Torr. The pure tin powder and nickel wire were used as starting materials. Substrates were cleaned by a conventional procedure and fixed onto a rotatable holder at a distance of 28 cm above the thermal evaporator. The film thickness and the deposition rate were controlled using a thickness monitor (LHC-2) with a quartz crystal microbalance. Then the deposited Sn films were thermally oxidized in air for 2 h at 400, 500, 600, 800 and 1000 °C, respectively. The oxidation temperature for the preparation of pure NiO films was selected to be 600 °C. It is known that the reaction of metallic Ni with O_2 to produce NiO is always accompanied with a small proportion of Ni_2O_3 formed at the temperature higher than 400 °C. However, Ni_2O_3 can be fully reduced to NiO at a temperature of 600 °C. Accordingly thermal deposited Ni films were thermally oxidized at 600 °C in a quartz tube under high purity oxygen for 2 h.

The composition and structure of the oxide films were examined using an X-ray diffractometer (Bruker Analytical X-ray systems, Germany) with Cu Kα radiation. Scanning electron microscopy (Philips XL30) was used to determine the film morphology and thickness, and the weight of the deposited film was estimated from the film thickness, area and density of metal oxides.

Electrochemical tests were carried out at room temperature with two electrode and three electrode cells, in which metallic lithium foils were used as both counter and reference electrodes, and the metal oxide films was used as a working electrode. The electrolyte was 1 M $LiPF_6$ dissolved in a 1:1 (w/w) mixture of ethyl carbonate (EC) and dimethyl carbonate (DMC) (Merck). The cells were discharged and charged at different current density in the range 10–80 μA cm^{-2} and cycled between 0.10 and 1.30 V versus Li/Li^+ for tin oxide film electrodes, as well as 0.01 and 3.0 V versus Li/Li^+ for nickel oxide film electrodes, respectively. Cyclic voltammograms were performed using CHI660A electrochemical workstation. Cells were assembled in an argon-filled glove box.

3. Results and discussion

3.1. Characterization of oxide films

Fig. 1 shows the XRD patterns of the tin oxide films on Si substrates fabricated at different oxidation temperatures. For the thin film fabricated at 400 °C, only diffraction peaks of SnO were observed. Upon heating the film to 500 °C, the diffraction peaks of SnO_2 appeared and there was only one (101) peak for SnO, indicating the crystalline of SnO_2 is formed along with a slight amount of SnO. According to the JCPDS reference (41–1445) the SnO_2 peaks at $2\theta = 26.61°$ (110), 33.89° (101), 37.95° (200) and 51.80° (211), correspond to typical cassiterite structure of SnO_2. It should be noted that the (101) peak of SnO becomes weaker with increasing the oxidation temperature. This implies that films fabricated at 500, 600 and 800 °C are composed of a mixture of SnO_2 and SnO. As the oxidation temperature up to 1000 °C diffraction peaks of SnO disappeared and the XRD pattern of the film coincides with that for tetragonal SnO_2. Additionally, the increase of the oxidation temperature leads to the increasing the sharpness of the diffraction peaks of SnO_2, indicating the growth of the crystallite size. In order to estimate the average size of crystallites, the Scherrer equation [15] was used with the width of the (101) peak of SnO and the (110) peak of SnO_2. The average crystallite sizes of the tin oxide films have been found to be

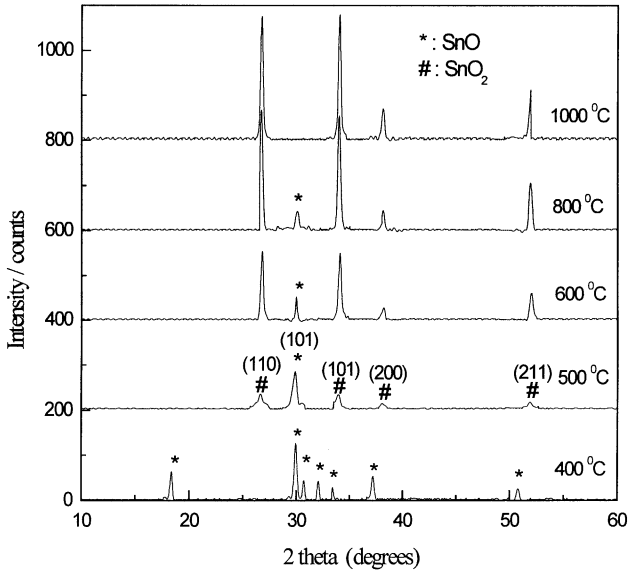

Fig. 1. X-ray diffraction patterns of tin oxides deposited on Si substrates fabricated at different oxidation temperatures for 2 h in air.

in the range 30–100 nm when the oxidation temperature increases from 400 to 1000 °C.

Fig. 2a and b presents SEM images of the SnO_x deposited on Si substrates fabricated at 600 and 800 °C, respectively. It can be seen that the thin film fabricated at 600 °C has an uniform distribution with the average particle size of 40–50 nm. As the oxidation temperature is increased to 800 °C, large particles are formed and their average size is found to be about 50–80 nm, which is close to that estimated from the XRD data.

XRD pattern of nickel oxide (NiO) thin film fabricated in oxygen at the oxidation temperature of 600 °C is illustrated in Fig. 3. The observed reflection peaks correspond very well to the bunsenite NiO phase. However, the relative intensities of the observed reflections are significantly different from those of bunsenite, in which the (012) peak is stronger than (101), indicating the formation of textured thin film. The average size of the NiO particles in the film is estimated to be around 30 nm from the Scherrer equation with the measured width of the (101) peak. SEM image of NiO at high magnification (40,000 times) shown in Fig. 2c indicates the compact structures of disordered particles with the size ranging from 30 to 100 nm.

The thickness and surface aspect of the thin films were also examined by SEM. The cross-sectional views of SnO_x and NiO films deposited on Si substrates fabricated at 600 °C are shown in Fig. 4a and b, respectively. It can be seen that the deposited oxide films are dense and smooth without any cracking. The thickness of the SnO_x and NiO thin film is estimated to be about 240 and 130 nm, respectively.

3.2. Cyclic voltammetry

The cyclic voltammograms (CVs) for the SnO and SnO_2 thin films fabricated at 400 and 1000 °C for the first five cycles at 0.1 mV s^{-1} are shown in Fig. 5a and b, respectively. It can be seen that there is a substantial difference between the first and the subsequent cycles. For SnO film electrode, the first cycle shows an irreversible reduction peak A with a maximum about 0.9 V, which disappears in the subsequent cycles. However, peaks B, B′ and C, C′ appear in all the five cycles, with minor shifting. Similar phenomenon was observed in the CVs of nano-sized SnO power electrode reported previously [16]. Peak A could be associated with the irreversible reactions including the reduction of electrolyte and the conversion reaction of SnO with metallic lithium into amorphous Li_2O and metallic tin. Peaks B/B′ and C/C′ could be due to the reversible alloying/dealloying process of Sn with Li [17]. For the SnO_2 film electrode, a broad irreversible reduction peak at around 0.6 V and an oxidation peak at about 0.7 V were observed in the first cycle only. These observations are similar to those of thin film crystalline SnO_2 electrode reported by Brousse et al. [9]. Obviously the irreversibility is more serious for SnO_2 film electrode than that for SnO electrode.

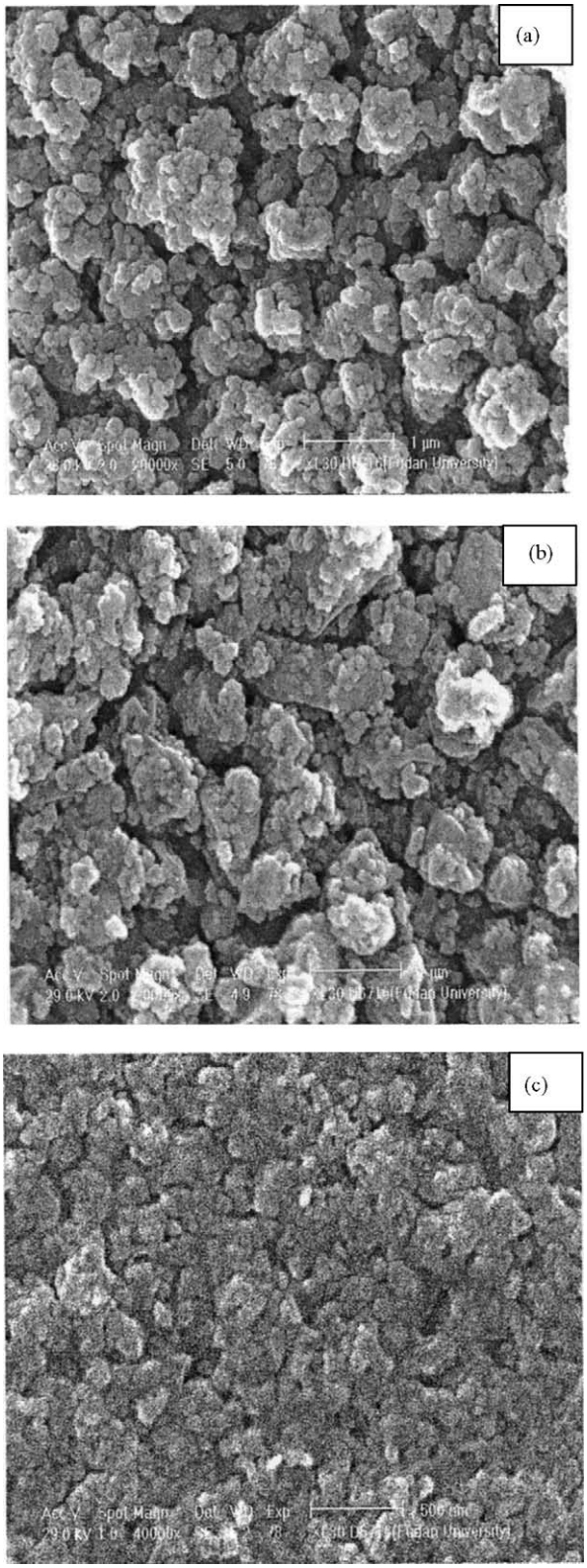

Fig. 2. Scanning electron microscopy micrographs of SnO_x deposited on Si substrates fabricated at (a) 600 °C, (b) 800 °C (magnified 20,000 times) and (c) NiO deposited on Si substrate fabricated at 600 °C (magnified 40,000 times).

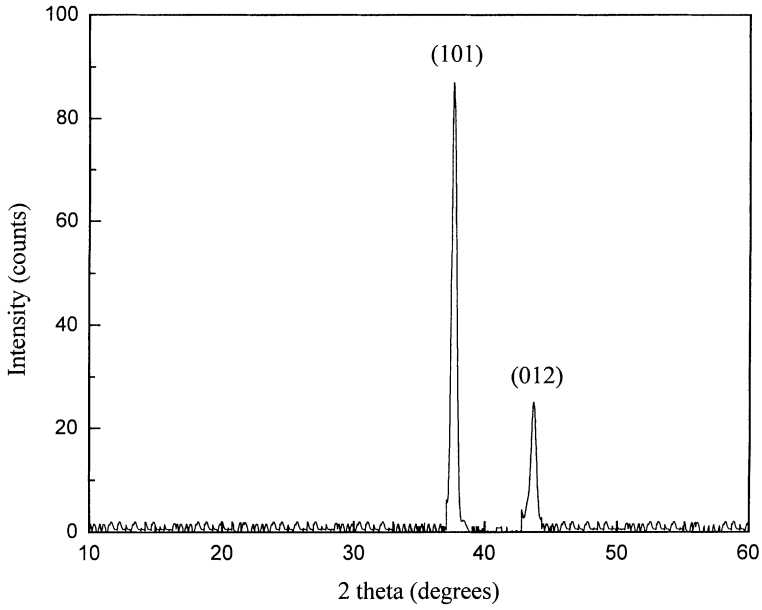

Fig. 3. X-ray diffraction pattern of NiO deposited on Si substrate fabricated at 600 °C for 2 h in oxygen.

Fig. 5c shows the CV curves of NiO film fabricated at 600 °C. The first cycle presents an irreversible reduction peak with a maximum about 0.34 V, which could be caused by the partially reversible electrochemical formation of SEI layer [18] and a reversible decomposition/formation reaction of NiO and metallic Ni nanoparticles [19]. The oxidation peaks around 1.75 V correspond to the reversible process from Ni to NiO and the decomposition of Li_2O in the subsequent cycles. The peak potentials slightly shift to 0.7 and 1.6 V, respectively. This behavior was also observed in the CVs of NiO film electrode prepared by reactive pulsed laser ablation [14].

3.3. Cycling behavior

The cycle performance of tin oxide film electrodes fabricated at different oxidation temperatures at a current density of 10 μA cm^{-2} is shown in Fig. 6. There is a large drop in the discharge capacity after the first cycle and the irreversible loss is as high as 30 and ∼40% for SnO film and SnO_2 film, respectively. The SnO film electrode has a reversible capacity of 825 mAh g^{-1} (the theoretical reversible capacity of SnO is 876 mAh g^{-1} [20]), which is much higher than the theoretical capacity of graphite, and 65% of the reversible capacity remained after 50 cycles. A reversible capacity of 760 mAh g^{-1} was obtained for SnO_2 film (the theoretical reversible capacity of SnO_2 is 783 mAh g^{-1} [20]) and 67% of the reversible capacity can be maintained over 50 cycles. As shown in the inset of Fig. 6, the SnO_x film electrode fabricated at 600 °C shows better performance than that fabricated at 800 °C in both the reversible capacity and capacity retention. At a high current density of 80 μA cm^{-2}, the SnO_x film electrode still retained satisfactory electrochemical performance with a reversible capacity

Table 1
Electrochemical properties of tin oxide and nickel oxide film electrodes fabricated by this work and other methods

Sample	Method	Initial capacity loss (mAh g^{-1})	10th discharge capacity (mAh g^{-1})	$R_{10/2}$ (%)	Voltage range (V)	Reference
SnO_x film	[a]	520	755	ca. 100	0.1–1.3	This work
SnO_2 film	PLD	590	467	ca. 100	0.1–1.2	[13]
SnO_2 film	CVD	600	500	ca. 100	0.05–1.15	[9]
SnO_2 film	EBE[b]	600	750	75	0.1–0.8	[11]
SnO_2 film	Sol–gel	900	500	83	0.05–1.2	[12]
NiO film	[a]	150	630	97	0.01–3.0	This work
NiO film	PLD	170	1278	85	0.01–3.0	[1]
NiO powder	–	350	570	95	0.01–3.0	[6]

$R_{10/2}$ is defined as the tenth/the second discharge capacity.
[a] Vacuum thermal evaporation and subsequent thermal oxidation.
[b] e-beam evaporation.

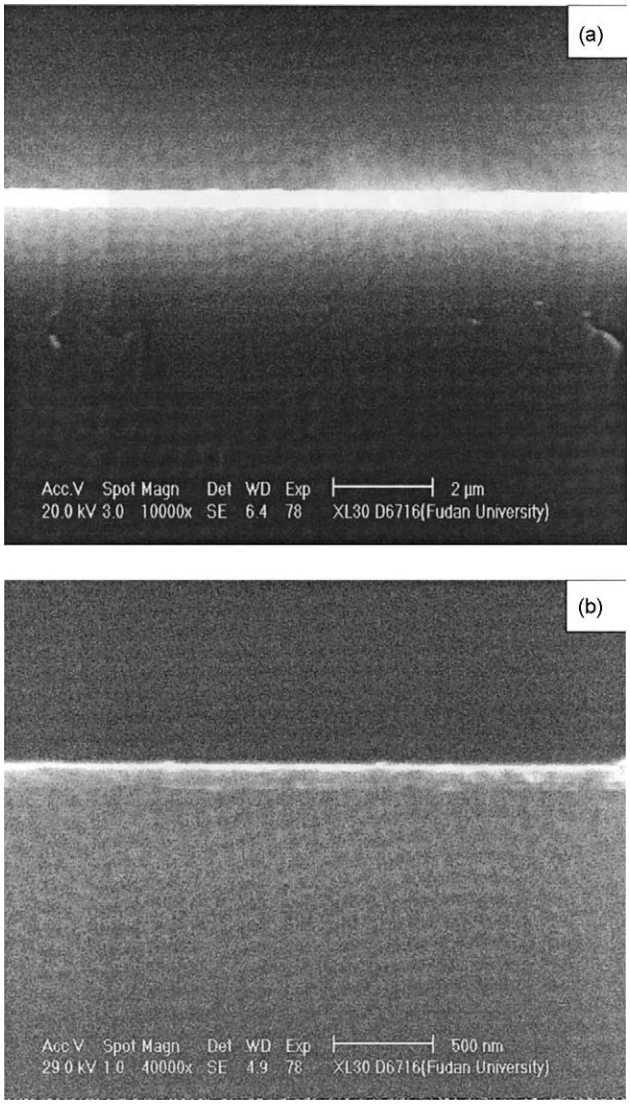

Fig. 4. SEM micrographs showing cross-sectional views of the films: (a) SnO_x deposited on Si substrate fabricated at 600 °C (magnified 10,000 times) and (b) NiO deposited on Si substrate fabricated at 600 °C (magnified 40,000 times).

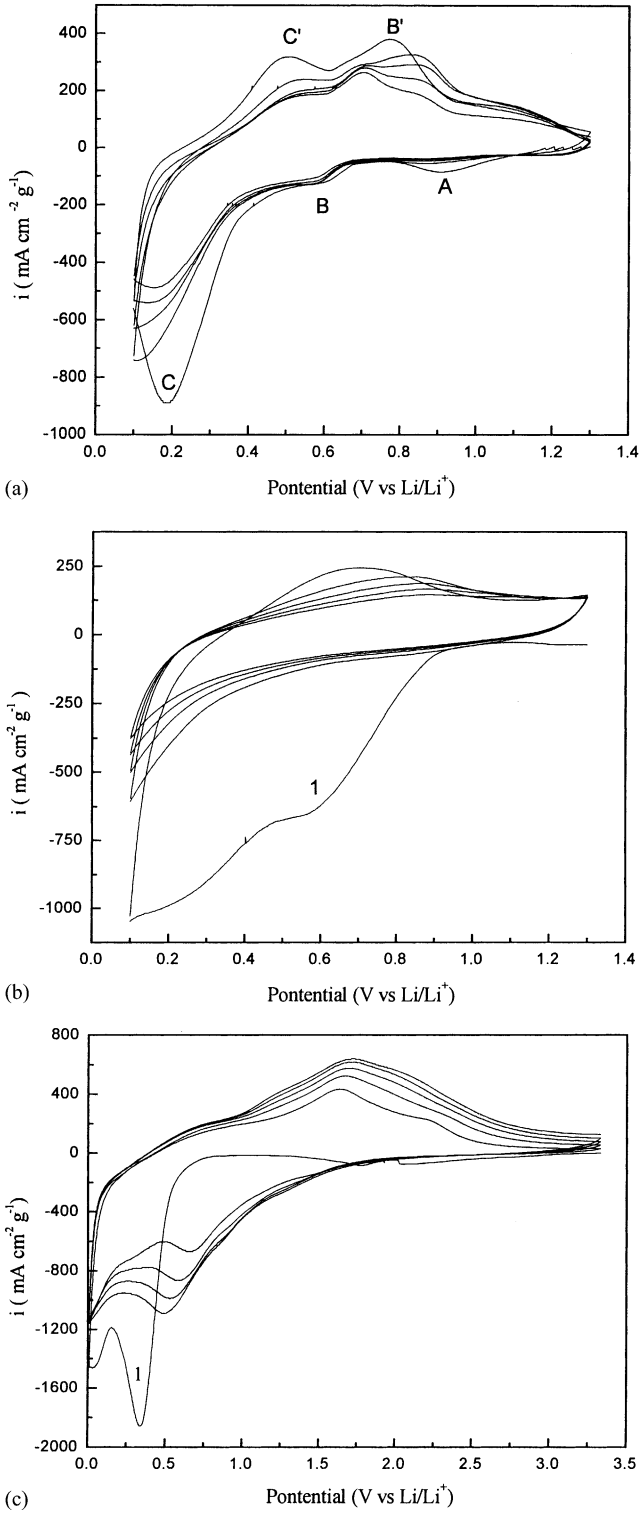

Fig. 5. Cyclic voltammograms of SnO, SnO_2 film electrodes fabricated at (a) 400 °C, (b) 1000 °C and (c) NiO film electrode fabricated at 600 °C for the first five cycles. Scanning rate: 0.1 mV s^{-1}.

of 700 mAh g^{-1} and a 70% of the capacity retention up to 50 cycles. These evidence showed that the capacity retention of SnO_x film electrodes improves as the particle size decreases, especially at high current density. Recently, Martin's group [5] reported that nano-structured tin oxide electrodes exhibiting the improved rate and cycling performance are related to the small size of the particles making up the electrode. It has been shown that the drawback for the tin oxides as anodes is its large volume changes occurring during the intercalation and deintercalation of Li^+ ions, which causes internal damage to the electrode and results in the loss of capacity and cyclability. However, tin oxide film electrodes composed of nanoparticles play critical roles in reducing this unwanted volume change and decomposition process. In addition, the tin oxide films prepared in this work are very thin with excellent uniformity. Thus, it is reasonable to suggest that very thin films composed of nanocrystalline tin oxides result in the better rate capacibility and higher specific capacity at high discharge rate.

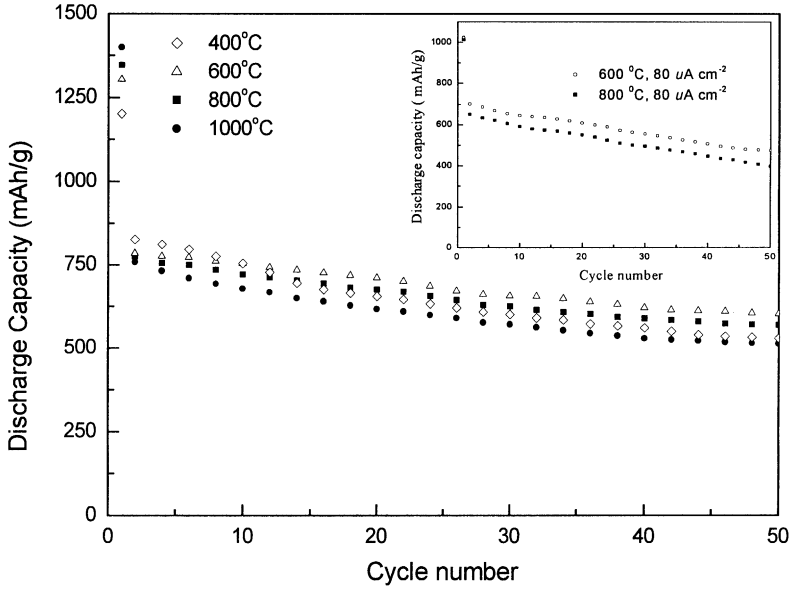

Fig. 6. Discharge capacity vs. cycle number for tin oxide film electrodes fabricated at different oxidation temperatures. Current density: 10 μA cm^{-2}. The inset is the cycle performance of SnO_x film electrodes fabricated at 600 and 800 °C at a current density of 80 μA cm^{-2}.

The electrochemical properties of the SnO_x film electrode fabricated at 600 °C and that of SnO_2 film electrodes reported in literatures [9,11–13] are summarized in Table 1. The reversible capacity of the film electrode prepared in this work is quite high and nearly the same as that of the SnO_2 film prepared by e-beam evaporation method [11]. Moreover, the cyclability of this film electrode is as good as the SnO_2 film prepared by CVD and PLD method [9,13].

Fig. 7 displays the first five discharge/charge curves of NiO film electrode fabricated at 600 °C. Despite the 20% irreversible loss observed between the first discharge and charge, the reversible capacity of NiO film anode is found to be 680 mAh g^{-1} (the theoretical value is 718 mAh g^{-1}) at a current density of 10 μA cm^{-2}. In the first discharge curve, a plateau range at 0.6–0.3 V can be observed, followed by a gradual decrease of potential down to 0.01 V. However, the subsequent discharge curves totally differ from that of the first one. In the second discharge, the plateau voltage increases and the amplitude of the plateau reduces obviously. There is no further change in the profiles for the subsequent cycles. These results are similar to those of the NiO power/Li cell reported previously [6].

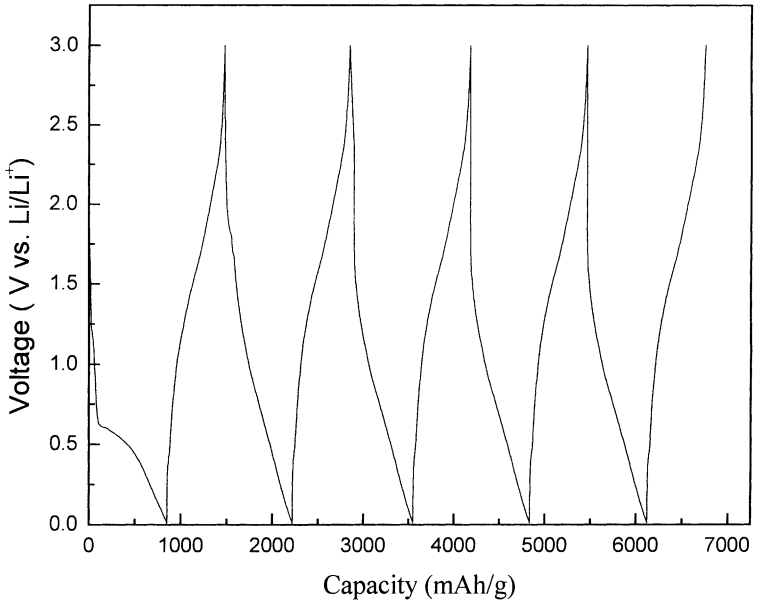

Fig. 7. The voltage–capacity profiles of the first five discharge/charge for NiO film electrode fabricated at 600 °C at a current density of 10 μA cm^{-2}.

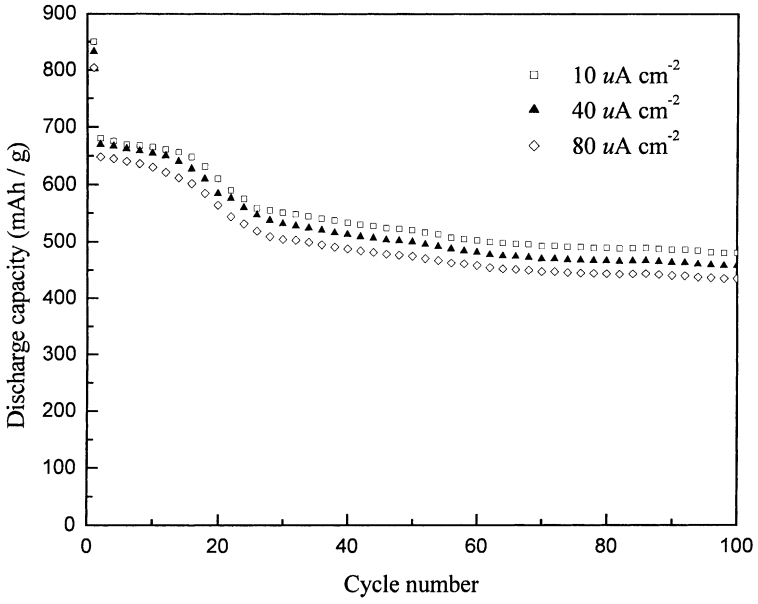

Fig. 8. Discharge capacity vs. cycle number for NiO film electrodes fabricated at 600 °C with different current densities.

Fig. 8 shows the cycle performance of the NiO film electrodes measured at different current densities. It can be seen that 70% of reversible capacity can be maintained over 100 cycles at 10 μA cm^{-2}, and the film electrode exhibits a 65% capacity retention up to 100 cycles at the current density as high as 80 μA cm^{-2}. The electrochemical properties of the NiO film electrode prepared in this work and that of NiO electrodes reported in literatures [6,14] are also listed in Table 1. Our film electrode exhibits better capacibility and higher reversible capacity. Tarascon and co-workers [6] reported that the reaction of NiO with lithium totally differs from the classical Li insertion/deinsertion process or Li-alloying reactions since metallic nickel cannot form alloys with lithium. It is most likely that the nano-sized Ni metal particles are formed from the starting nanocrystalline NiO during the first discharge, then the high reactive nickel nanoparticles could convert back to NiO accompanying the decomposition of Li_2O upon the charging process.

4. Conclusions

Nanocrytalline tin oxides (SnO, SnO_2 and SnO_x) and NiO thin films have been successfully deposited on the stainless-steel substrate by vacuum thermal evaporation and subsequent thermal oxidation in air and oxygen ambient, respectively. XRD, SEM and electrochemical measurements showed that the SnO_x film electrodes fabricated at 600 and 800 °C are composed of nanocrystalline SnO and SnO_2, and these film electrodes have better cycling performance than SnO film and SnO_2 film electrodes fabricated at 400 and 1000 °C, respectively. Compared with the tin oxide film electrodes, NiO film electrodes are found to sustain better rate capability. Our results demonstrate that vacuum thermal evaporation and subsequent thermal oxidation could be a simple and promising method to fabricate smooth, pin-hole free and dense metal oxide thin film electrodes for the all-solid-state Li-ion batteries.

Acknowledgements

This work is supported by the National Nature Science Foundation of China (Project No. 200083001). Authors thank Professor Qike Zheng for her helpful discussions.

References

[1] Fuji Photo Film Co. Ltd., European Patent 0,651,450,A1 (1995).
[2] I.A. Courtney, J.R. Dahn, J. Electrochem. Soc. 144 (1997) 2045.
[3] J.O. Besenhard, J. Yang, M. Winter, J. Power Sources 68 (1997) 87.
[4] I.A. Courtney, J.R. Dahn, J. Electrochem. Soc. 144 (1997) 2943.
[5] N. Li, C.R. Martin, B. Scrosati, J. Power Sources 97–98 (2001) 240.
[6] P. Poizot, S. Laruelle, S. Grugeon, L. Dupont, J.-M. Tarascon, Nature 407 (2000) 496.
[7] W.H. Lee, H.C. Son, H.S. Moon, Y.I. Kim, S.H. Sung, J.Y. Kim, J.G. Lee, J.W. Park, J. Power Sources 89 (2000) 102.
[8] H. Huang, E.M. Kelder, L. Chen, J. Schoonman, J. Power Sources 81–82 (1999) 362.
[9] T. Brousse, R. Retoux, U. Hertench, D.M. Schleich, J. Electrochem. Soc. 145 (1998) 1.
[10] S.C. Nam, C.H. Paik, W.I. Cho, B.W. Cho, H.S. Chun, K.S. Yun, J. Power Sources 84 (1999) 24.
[11] Y.I. Kim, C.S. Yoon, J.W. Park, J. Solid State Chem. 160 (2001) 388.

[12] J. Santos-Pena, T. Brousse, L. Sanchez, J. Morales, D.M. Schleich, J. Power Sources 97–98 (2001) 232.
[13] F. Ding, Z.W. Fu, M.F. Zhou, Q.Z. Qin, J. Electrochem. Soc. 146 (1999) 3554.
[14] Y. Wang, Q.Z. Qin, J. Electrochem. Soc. 149 (2002) A873.
[15] B.D. Cullity, Elements of X-ray Diffraction, 2nd ed., Addison-Wesley, Reading, MA, 1978.
[16] J.Z. Li, H. Li, Z.X. Wang, X.J. Huang, L.Q. Chen, J. Power Sources 81–82 (1999) 346.
[17] M. Mohamedi, S.-J. Lee, D. Takahashi, M. Nishizawa, T. Itoh, I. Uchida, Electrochim. Acta 46 (2001) 1161.
[18] S. Grugeon, S. Laruelle, R. Herrera-Urbina, L. Dupont, P. Poizot, J.-M. Tarascon, J. Electrochem. Soc. 148 (2001) A285.
[19] P. Poizot, S. Laruelle, S. Grugeon, L. Dupont, J.-M. Tarascon, J. Power Sources 97–98 (2001) 235.
[20] J. Read, D. Foster, J. Wolfenstine, W. Behl, J. Power Sources 96 (2001) 277.